Table S1. Correlation coefficients between the tree–ring width chronologies from the two study sites, BYS and LCM, over their common period when EPS larger than 0.85.

Chronologies	Detrending method		
	NELR	SP67	SPA50
EWW STD	0.8 (1888) / 0.78 (1889)	0.82 (1888) / 0.8 (1889)	0.82 (1888) / 0.8 (1889)
LWW STD	0.65 (1892) / 0.67 (1897)	0.73 (1907) / 0.69 (1912)	0.67 (1892) / 0.63 (1897)
TRW STD	0.76 (1884) / 0.72 (1888)	0.8 (1887) / 0.76 (1892)	0.80 (1887) / 0.76 (1892)
EWW SSF	0.79 (1888) / 0.78 (1889)	0.76 (1888) / 0.77 (1889)	0.81 (1888) / 0.78 (1889)
LWW SSF	0.67 (1892) / 0.68 (1897)	0.58 (1892) / 0.62 (1897)	0.63 (1896) / 0.64 (1901)
TRW SSF	0.74 (1884) / 0.72 (1888)	0.74 (1887) / 0.73 (1892)	0.76 (1884) / 0.74 (1889)

Note: The correlation coefficients before (after) the slashes are for the original (prewhitened and linearly detrended) STD and SSF chronologies. All correlation coefficients are statistically significant at the 0.001 level. The beginning year of the common period was shown in the bracket. The ending year for all chronologies was 2005.

Table S2. Descriptive statitics of the composite STD and SSF tree–ring width chronologies.

Detrending method	Chronology	Starting year when EPS > 0.85	Standard deviation	Mean sensitivity	First-order autocorrelation
NELR	EWW STD	1864	0.232	0.217	0.306
	LWW STD	1871	0.25	0.219	0.358
	TRW STD	1864	0.216	0.194	0.389
SP67	EWW STD	1864	0.232	0.218	0.29
	LWW STD	1871	0.249	0.229	0.313
	TRW STD	1864	0.215	0.196	0.363
SPA50	EWW STD	1864	0.232	0.218	0.281
	LWW STD	1871	0.248	0.227	0.301
	TRW STD	1859	0.214	0.196	0.354
NELR	EWW SSF	1864	0.237	0.218	0.346
	LWW SSF	1865	0.265	0.221	0.438
	TRW SSF	1859	0.222	0.193	0.44
SP67	EWW SSF	1864	0.24	0.217	0.348
	LWW SSF	1867	0.257	0.229	0.362
	TRW SSF	1864	0.222	0.197	0.403
SPA50	EWW SSF	1864	0.234	0.207	0.353
	LWW SSF	1868	0.252	0.223	0.357
	TRW SSF	1859	0.216	0.192	0.378

Table S3. Statitics of the detrended ring-width series over their common period 1915–2005.

Detrending method	Chronology	PC1	Rbar	SNR	EPS
NELR	EWW STD	0.386	0.362	31.187	0.969
	LWW STD	0.328	0.298	23.303	0.959
	TRW STD	0.384	0.356	30.453	0.968
SP67	EWW STD	0.427	0.408	37.948	0.974
	LWW STD	0.353	0.326	26.594	0.964
	TRW STD	0.422	0.399	36.495	0.973
SPA50	EWW STD	0.411	0.391	35.311	0.972
	LWW STD	0.341	0.314	25.203	0.962
	TRW STD	0.404	0.38	33.745	0.971
NELR	EWW SSF	0.399	0.375	32.991	0.971
	LWW SSF	0.317	0.285	21.911	0.956
	TRW SSF	0.393	0.359	31.249	0.969
SP67	EWW SSF	0.453	0.436	42.488	0.977
	LWW SSF	0.366	0.339	28.266	0.966
	TRW SSF	0.441	0.42	39.817	0.976
SPA50	EWW SSF	0.474	0.458	46.418	0.979
	LWW SSF	0.352	0.326	26.637	0.964
	TRW SSF	0.431	0.409	38.087	0.974

Note: The common period for the tree–ring width dataset is calculated with the “common.interval” function in R package “dplR” (https://r-forge.r- project.org/projects/dplr/) based on a trade–off between the maximum number of series and years. The statistics, PC1, Rbar, SNR, and EPS represent the first principal component, mean interseries correlation between all series, signal–to–noise ratio, and expressed population signal, respectively.

Table S4. The meterological stations utilized by CRU dataset (http://www.cru.uea.ac.uk/data) located in the area between latitudes 32° N and 34.5° N, and longitudes 111° E and 112° E.

Meteorological station	Longitude (°E)	Latitude (°N)	Climate factor	Temporal cover
Lushi	111.03	34.05	Precipitation	1952.07–2013.12
			Temperature	1952.07–2016.12
Laohekou	111.73	32.43	Precipitation	1933.02–1933.11; 1934.01–1935.06; 1935.08–1935.12; 1936.08–1938.07; 1950.06–2005.06; 2005.08–2013.12
			Temperature	1951.01–2016.12
Yunxian	111.8	32.9	Precipitation	1933.03–1938.05; 1938.07–1947.10; 1950.03–1990.12; 1991.05; 1991.07–1991.08

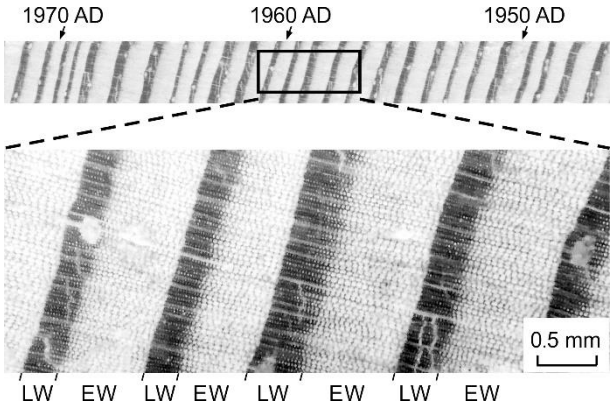

Figure S1. Scanned photograph of a section of *P. tabulaeformis* tree–ring sample (LCM0118A). The distinct earlywood (EW) and latewood (LW) segments can be identified by inspection under a microscope.

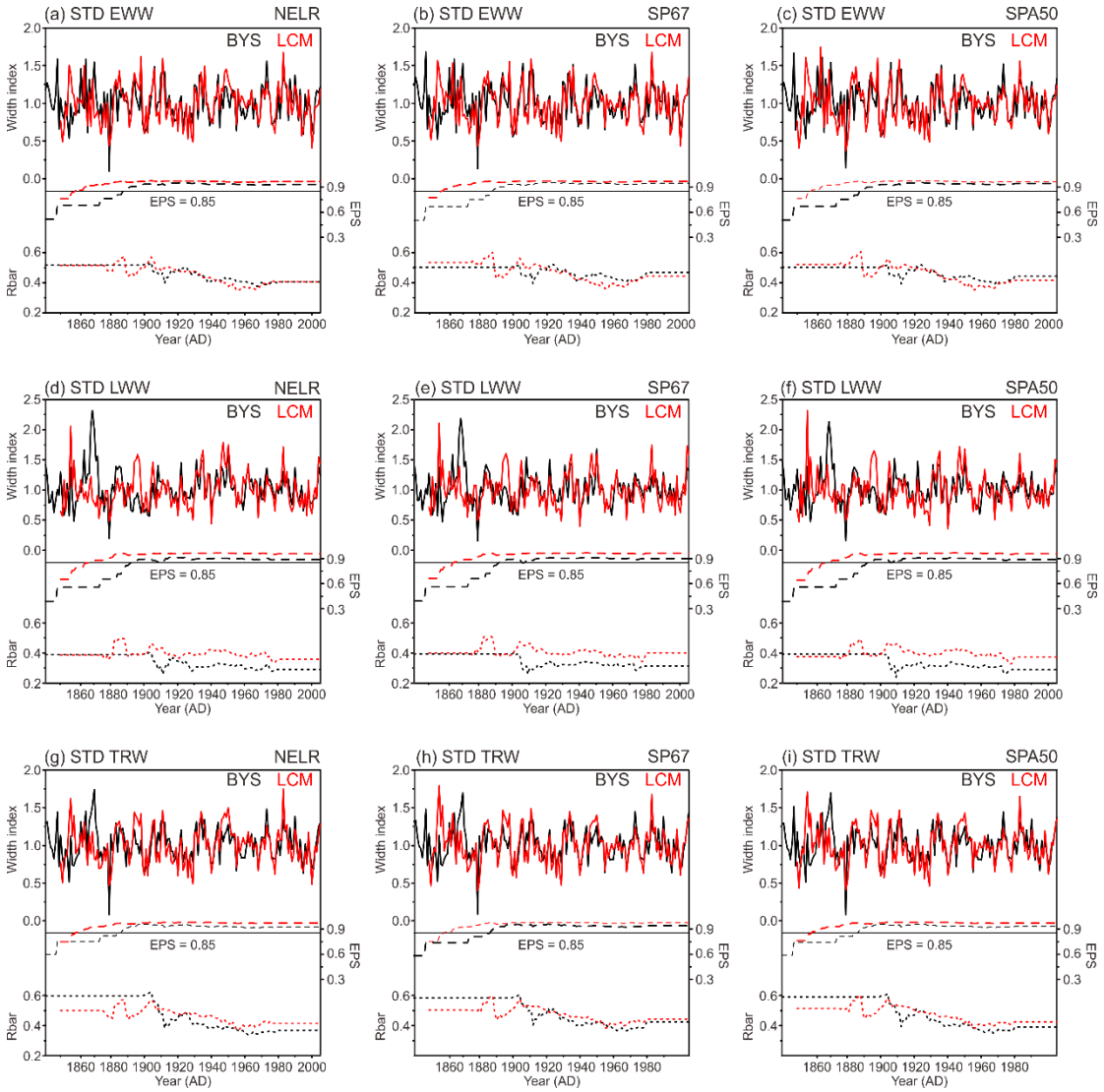

Figure S2. Standard tree-ring width chronologies (solid curve) generatued using three kinds of detrending methods for **(a–c)** earlywood width (EWW), **(d–f)** latewood width (LWW), and **(g–i)** total tree–ring width (TRW) at the two study sites, BYS (black) and LCM (red). The three kinds of detrending methods are: (1) negative exponential function together with linear regression with negative (or zero) slope (NELR), (2) cubic smoothed splines with a 50 % frequency cutoff of 67 % of the series length (SP67), and (3) age-dependent splines with an initial stiffness of 50 years (SPA50). The dashed and dotted curves denote the running expressed population signal (EPS) and Rbar values, respectively. The horizontal line indicates the threshold EPS value of 0.85. The running EPS and Rbar values were calculated over a 51–year window.

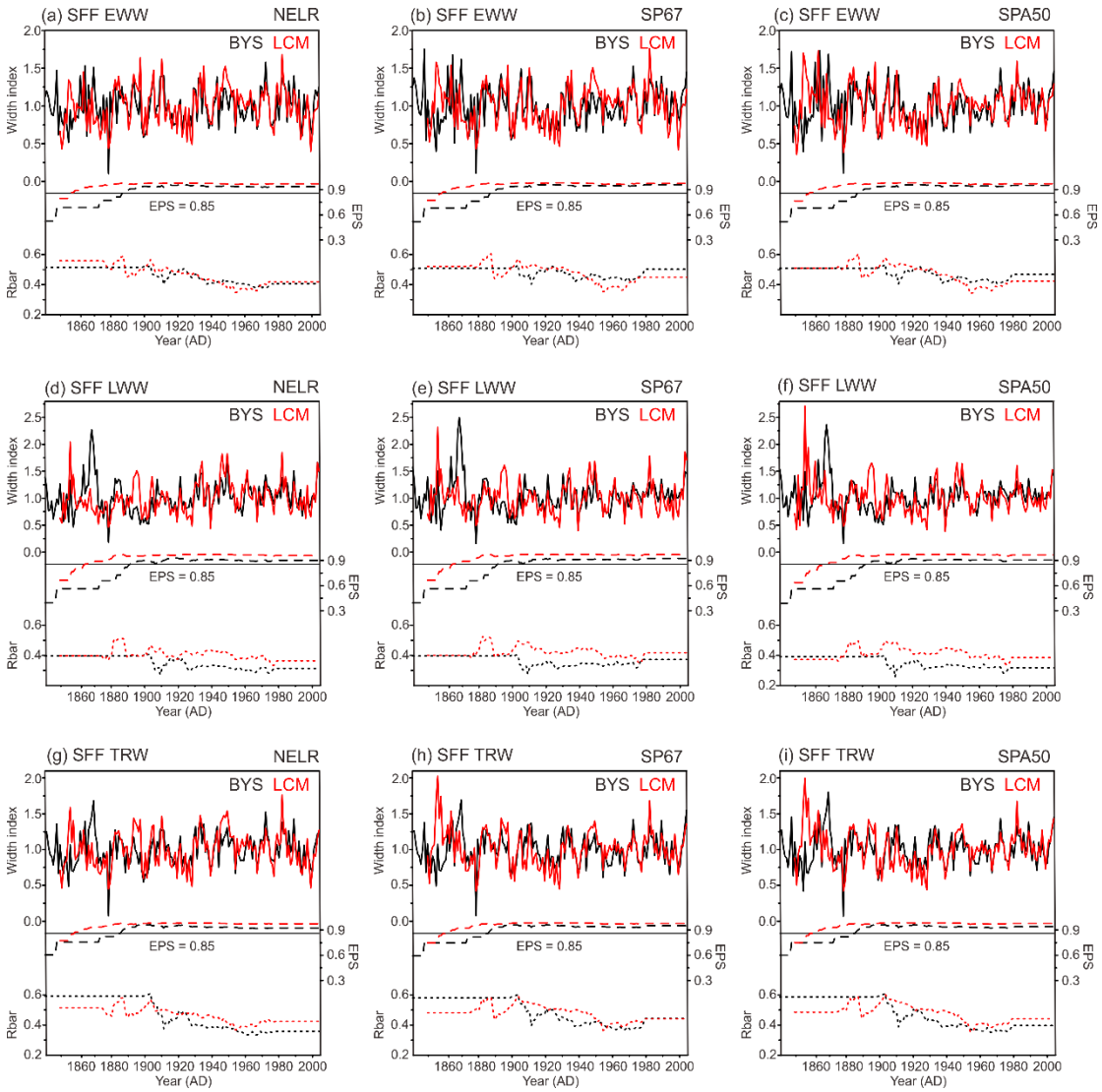

Figure S3. The same as Figure S2, but for the signal-free (SSF) chronologies.

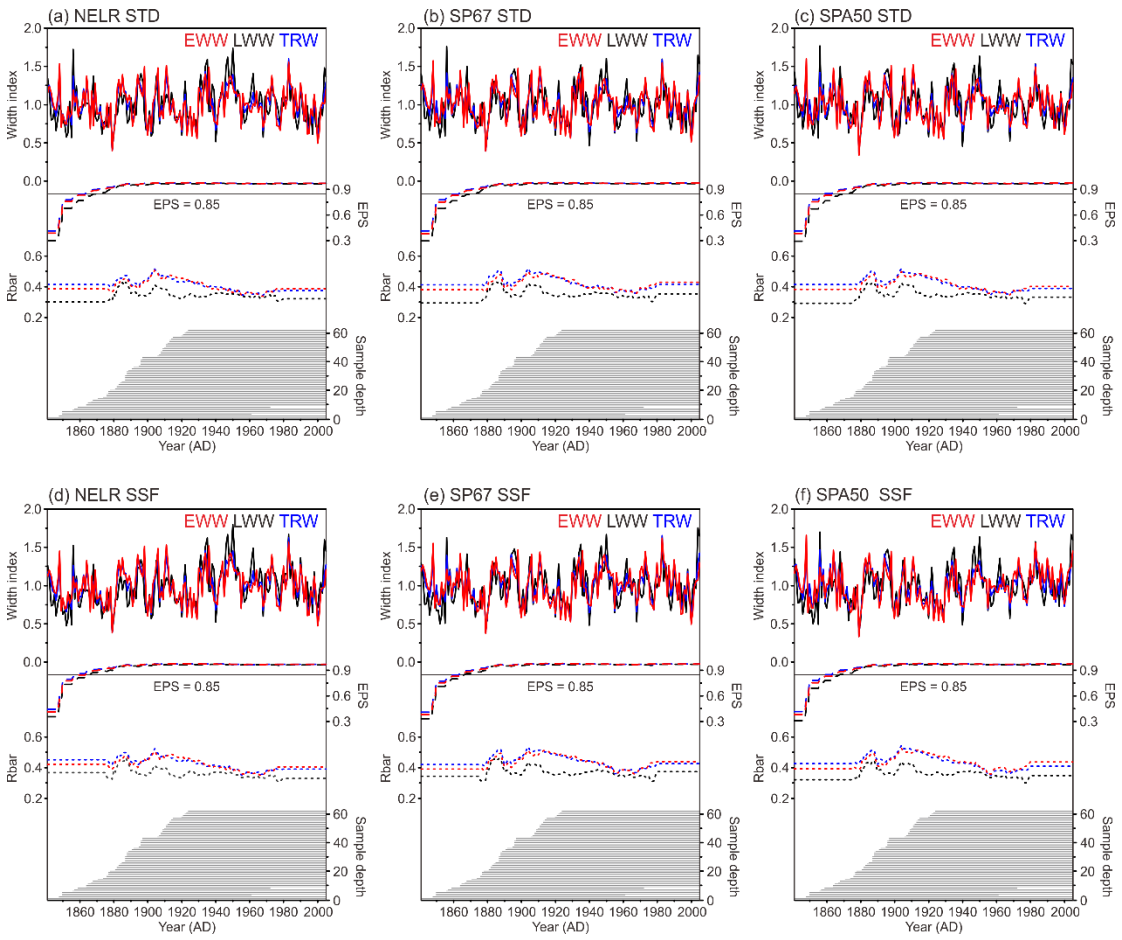

Figure S4. Composite STD **(a–c)** and SSF (**d–f**) tree-ring width chronologies for EWW (red), LWW (black), and TRW (blue) generated using the merged tree–ring samples from the two study sites, BYS and LCM, based on three kinds of detrending methods. The detrending methods are: (1) negative exponential function together with linear regression with negative (or zero) slope (NELR), (2) cubic smoothed splines with a 50 % frequency cutoff of 67 % of the series length (SP67), and (3) age-dependent splines with an initial stiffness of 50 years (SPA50). The dashed and dotted curves denote the running expressed population signal (EPS) and Rbar values, respectively. The horizontal line indicates the threshold EPS value of 0.85. The running EPS and Rbar values were calculated over a 51–year window. The segement plot indicated the sample depth.

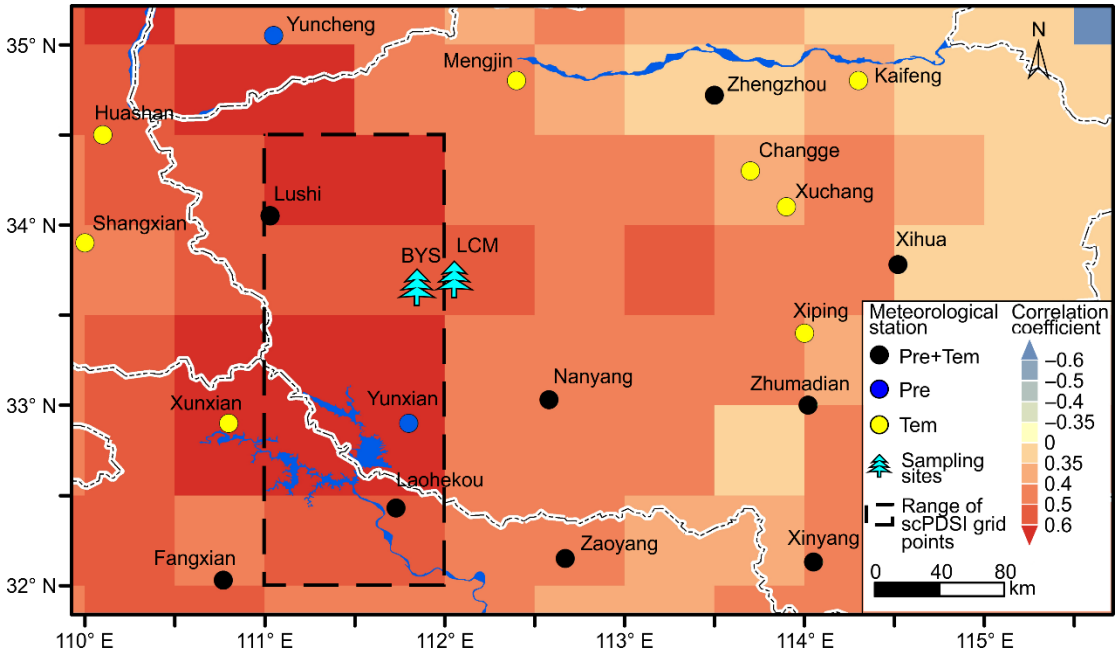

Figure S5. Spatial distribution of the meteorological stations included in the CRU dataset (http://www.cru.uea.ac.uk/data) around the tree-ring sampling sites, BYS and LCM. Black cycles represent the meteorological stations that provide both precipitation and temperature data. While, blue (yellow) cycles represent those that only provide precipitation (temperature) data. The dashed rectangle indicates the range of scPDSI grid points used for calibration in this study. The color patches denote the spatial correlation coefficients between May-July scPDSI and NELR based EWW STD chronology.

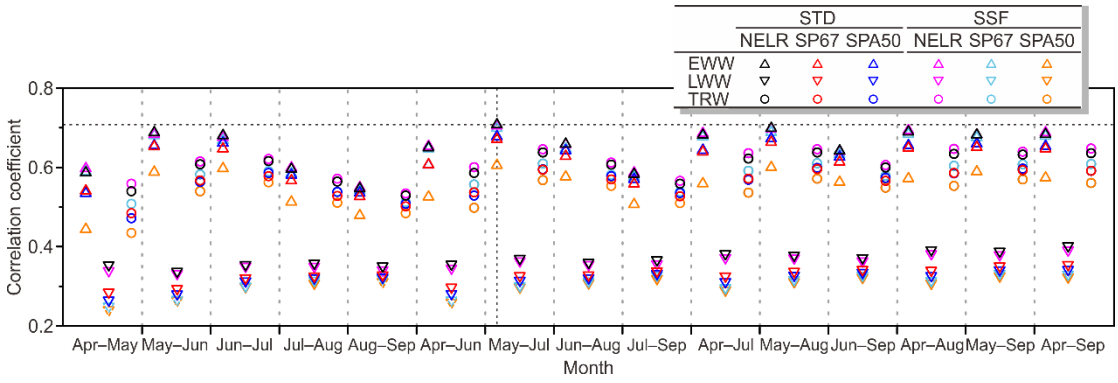

Figure S6. Correlation coefficients between the tree-ring width chronologies and multi-month averaged scPDSI (April to September of the current year). The up triangle, down triangle, and circle indicate the chronologies of EWW, LWW, and TRW, respectively. The color black, red and blue indicate the STD chronologies generated using the detrending methods NELR, SP67, and SPA50, respectively. The color magenta, cyan, and orange indicate the SSF chronologies generated using the detrending methods NELR, SP67, and SPA50, respectively. The dashed symbol indicates that the correlation does not reach the 0.05 significance level, which were tested using the Monte Carlo method (Efron and Tibshirani, 1986; Macias-Fauria et al., 2012).

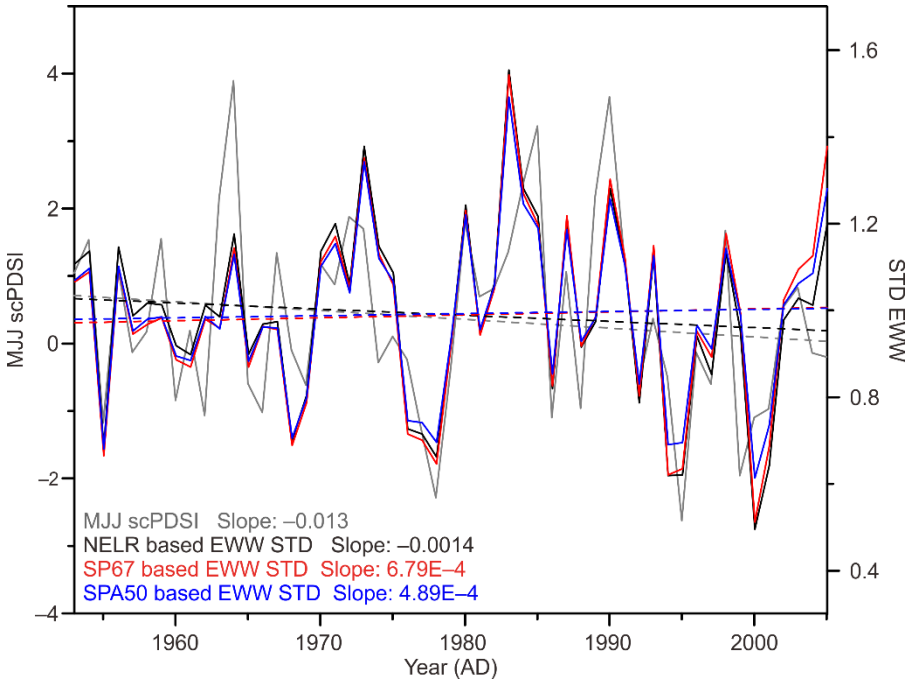

Figure S7. Comparisons between the MJJ scPDSI (gray) and EWW STD chronologies generated using the detrending methods NELR (black), SP67 (red), and SPA50 (blue) during the period 1953–2005. The corresponding linear trends were indicated by the dashed lines, and the slope statistics were labelled in the bottom left corner of the figure.

References

Efron, B., and Tibshirani, R.: Bootstrap methods for standard errors, confidence intervals, and other measures of statistical accuracy, Stat. Sci., 1, 54–77, 1986.

Macias-Fauria, M., Grinsted, A., Helama, S., and Holopainen, J.: Persistence matters: Estimation of the statistical significance of paleoclimatic reconstruction statistics from autocorrelated time series, Dendrochronologia, 30, 179–187, https://doi.org/10.1016/j.dendro.2011.08.003, 2012.